CogWave: Open-source Software Framework for Cognitive Radio Waveform Design

Dr Vincent Le Nir
Royal Military Academy - Department CISS
Dr Bart Scheers
Royal Military Academy – Department CISS
BELGIUM
vincent.lenir@rma.ac.be
bart.scheers@rma.ac.be

ABSTRACT

CogWave is an open-source software framework aiming at developing cognitive radio (CR) waveforms. Multiple waveforms have been implemented in CogWave, such as the multichannel DAA-OFDM waveform, the DADS waveform, and GNU Radio waveforms. CogWave provides the means to implement different CR waveforms and to develop rules to switch between different CR waveforms during run-time according to the user needs and the electromagnetic environment. A description of a CR demonstrator is given, in which a jammer perturbs the data transmission between two CR nodes. It is shown that when the throughput drops under a predefined threshold, the CR nodes switch from the DADS to the multichannel DAA-OFDM automatically while maintaining communication.

1. Introduction

The concept of cognitive radio (CR) is to have a network of software defined radios (SDRs) which can autoconfigure and autonomously change its parameters (waveform, frequency, bandwidth, power) according to the user needs and the electromagnetic environment [1]. CogWave is an open-source software framework aiming at developing cognitive radio (CR) waveforms [2]. CogWave uses the Qt framework, the communications library IT++, the USRP universal hardware driver (UHD) and other libraries to enable real-time transmission between USRP devices. Multiple waveforms have been implemented in CogWave. The first waveform is the multichannel orthogonal frequency division multiplexing (OFDM) waveform with detection and avoid (DAA) introduced in [3]. The second waveform is the delay and add direct sequence (DADS) waveform with a short spreading sequence introduced in [4]. Other waveforms such as OFDM, BPSK, QPSK, GMSK, CPFSK etc. have been ported to CogWave from GNU Radio [5]. A CR node is composed of a host PC running the CogWave framework and a USRP. CogWave gives the ability to the CR nodes to modify the waveform and its parameters during run-time according to the user needs and the electromagnetic environment. This paper gives a description of CogWave and a CR demonstrator in which a jammer perturbs the data transmission between two CR nodes. It is shown that when the throughput drops under a predefined threshold, the CR nodes switch from the DADS to the multichannel DAA-OFDM automatically while maintaining communication. Section II provides a description of the CogWave framework and two waveforms, i.e. the multichannel DAA-OFDM waveform and the DADS waveform. A description of the CR demonstrator and results are given in Section III. Section IV concludes this paper.

2. Description of CogWave framework

This Section provides a description of the CogWave framework. The main objective of CogWave is to develop a library of waveforms and to develop rules to switch between these waveforms during run-time

according to the user needs and the electromagnetic environment. Multiple waveforms have been implemented in CogWave. The first waveform is the multichannel DAA-OFDM waveform introduced in [3]. The multichannel DAA-OFDM waveform uses energy-based sensing to adjust dynamically the channel and to mitigate interference. It has no pilot symbols and requires blind time, frequency and phase recovery. The second waveform is the DADS waveform with a short spreading sequence introduced in [4]. The DADS waveform has a very low complexity and does not require frequency and phase recovery. Other waveforms such as OFDM, BPSK, QPSK, GMSK, CPFSK etc. have been ported from GNU Radio [5]. Either a frequency division duplex (FDD) or a time division duplex (TDD) mode can be used for all waveforms. In a TDD mode, a frame is composed of two slots to transmit and receive packets on the same frequency. In a FDD, mode, a frame is composed of a single slot to transmit and receive packets on different frequencies. Frequency hopping can be enabled by a predefined hopping sequence only known to the CR nodes. The USRP RF frontend allows to perform frequency hopping over a large frequency range from 70 MHz to 6 GHz.

Figure 1 Data packet in CogWave
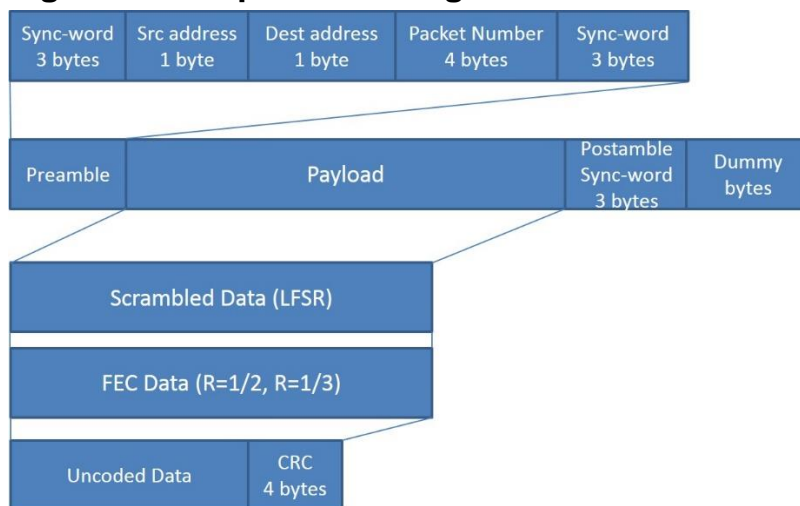
A slot has a fixed duration in order to carry a modulated data packet of variable size as described in Figure 1. Modulated dummy bytes are used to fill the slot period. Frame synchronization uses sync-words. The uncoded data is processed by cyclic redundancy check (CRC), forward error correction (FEC) and linear feedback shift register (LFSR) scrambling. This uncoded data can be received and transmitted to virtual network interfaces (TUN/TAP) to establish connections between CR nodes. This uncoded data can also be received and transmitted to named pipes for simple text messaging, video and audio streaming, or even in the case of hardware-in-the-loop network simulation/emulation/testbed with more complex frameworks such as OMNeT++ and ns-3 [6], [7]. Such frameworks allow to create CR nodes with a complete protocol stack from the MAC up to the application layer independently of the CogWave PHY layer.

2.1. Description of the multichannel DAA-OFDM waveform

The multichannel DAA-OFDM waveform has been introduced in [3]. The band of interest B is composed of N OFDM sub-carriers and is divided into a number of channels S of width B/S. Each channel is composed of N/S OFDM sub-carriers. A CR node determines which channel has the lowest energy every frame's period by

$$S_{opt} = \min_{m} \sum_{i=\frac{mN}{S}}^{\frac{(m+1)N}{S}-1} E(i)$$

with $m = [0, ..., S-1]$ in which $E(i)$ is the averaged periodogram of sub-carrier i given by

$$E(i) = \frac{1}{KN} \sum_{k=0}^{K-1} \left| \sum_{n=0}^{N-1} y(kN+n) e^{-\frac{j2\pi in}{N}} \right|^2$$

with $i = [0, ..., N-1]$ sub-carriers in which $y(kN+n)$ with $k = [0, ..., K-1]$, $n = [0, ..., N-1]$ are the received complex samples for a slot period in the band of interest. A CR node OFDM-modulates the bit sequence on the channel which has the lowest energy. In a TDD mode, if a packet was received correctly on another channel, the same channel is used to OFDM-modulate the bit sequence. A CR node performs an OFDM signal detection and time recovery by the cyclic prefix based sliding window metric [8] given by

$$\rho(\theta) = \frac{\left| \sum_{k=0}^{K-2} \sum_{j=\theta}^{\theta+P-1} y(k(N+P)+j) y^*(k(N+P)+j+N) \right|}{(K-1)P\sigma_y^2}$$

with P the cyclic prefix size. The time offset estimate is given by

$$\theta^{opt} = \max_{\theta \in \{0,...,N+P-1\}} \rho(\theta)$$

In order to allow the detection of an OFDM signal even in the presence of an unknown signal, the CR node uses a detection threshold based on the non-correlated part of the cyclic prefix based sliding window metric at the time offset estimate instead of the noise variance [3]. The non-correlated part of the cyclic prefix based sliding window metric at the time offset estimate is given by the vector $\left[\rho\left(mod(\theta^{opt} + 2P, N+P) \right), ..., \rho\left(mod(\theta^{opt} + N - P - 1, N+P) \right) \right]$. Assuming that the non-correlated part is a Gaussian distribution with mean m_{nc} and variance σ_{nc}^2, the detection threshold η is given by

$$η = m_{nc} + \alpha \sigma_{nc}$$

with α an integer corresponding to the number of standard deviations necessary to discriminate between the cyclic prefix based sliding window metric at the time offset estimate $\rho(\theta^{opt})$ and its non-correlated part $\left[\rho\left(mod(\theta^{opt} + 2P, N+P) \right), ..., \rho\left(mod(\theta^{opt} + N - P - 1, N+P) \right) \right]$. The detector scheme is

$$\rho(\theta^{opt}) > η \quad Presence \ of \ an \ OFDM \ signal$$
$$\rho(\theta^{opt}) < η \quad Absence \ of \ an \ OFDM \ signal$$

The CR node also use the cyclic prefix based sliding window time offset estimate to estimate the frequency offset (ϵ^{opt}) for carrier frequency recovery [9]

$$\epsilon^{opt} = -\frac{1}{2\pi N} \angle \rho(\theta^{opt})$$

After time and frequency offset corrections, the OFDM symbols are transformed to the frequency domain by the discrete Fourier transform (DFT) operation. As there is no interference between two consecutive

OFDM symbols, independent sub-carriers are obtained with the following channel model

$$Y(kN + i) = H(kN + i)X(kN + i) + N(kN + i)$$

with $k = [0, ..., K - 1]$ and $i = [0, ..., N - 1]$, in which $Y(kN + i)$, $H(kN + i)$, $X(kN + i)$, and $N(kN + i)$ are respectively the demodulated data, the channel frequency response, the transmitted symbol and the noise for the block k and sub-carrier i. Assuming the channel amplitude invariant over the K blocks, a blind estimate of the channel amplitude for automatic gain control is given by

$$|H(i)^{opt}| = \frac{1}{K} \sum_{k=0}^{K-1} |Y(kN + i)|^2$$

Figure 2 Blind carrier phase recovery for multichannel DAA-OFDM

Algorithm 1 Amplitude Gain Control and Carrier phase recovery with the M-power estimators

1   $\phi(i)^{est} = \angle \frac{1}{K} \sum_{k=0}^{K-1} Y(kN + i)^M \; \forall i$

2   $\phi(0)^{opt} = \phi(0)^{est}$

3   for $i = 1$ to $N - 1$

4   if $|\phi(i)^{est} - \phi(i - 1)^{est}| > \frac{\pi}{M}$

5       $\phi(i)^{opt} = |\phi(i)^{est} - \phi(i - 1)^{est}| - \frac{2\pi}{M}$

6   else

7       $\phi(i)^{opt} = \phi(i)^{est} - \phi(i - 1)^{est}$

8     $\phi(i)^{opt} = \phi(i)^{opt} + \phi(i - 1)^{opt}$

9   end for

10   $Y(kN + i) = \frac{1}{|H(i)^{opt}|} Y(kN + i) e^{-j\phi(i)^{opt}} \; \forall k, i$

11   $\phi(k)^{est} = \angle \frac{1}{N} \sum_{i=0}^{N-1} Y(kN + i)^M \; \forall k$

12   $\phi(0)^{opt} = \phi(0)^{est}$

13   for $k = 1$ to $K - 1$

14   if $|\phi(k)^{est} - \phi(k - 1)^{est}| > \frac{\pi}{M}$

15       $\phi(i)^{opt} = |\phi(i)^{est} - \phi(i - 1)^{est}| - \frac{2\pi}{M}$

16   else

17       $\phi(k)^{opt} = \phi(k)^{est} - \phi(k - 1)^{est}$

18     $\phi(k)^{opt} = \phi(k)^{opt} + \phi(k - 1)^{opt}$

19   end for

20 $Y(kN + i) = Y(kN + i) e^{-j\phi(k)^{opt}} \; \forall k, i$

The channel phase varies between sub-carriers due to an incorrect time offset estimate and the channel frequency response. The channel phase also varies between blocks in time due to a remaining frequency offset or oscillator phase noise. The two-dimensional carrier phase recovery given by Algorithm 1 uses the second-power estimator for the BPSK constellation ($M = 2$) and the fourth-power estimator for QAM constellations ($M = 4$) [10], [11]. A 1-D phase unwrapping is performed in the frequency domain to correct linear shifts of the phase in the frequency domain due to an incorrect time offset as well as abrupt

changes of the phase due to the phase ambiguity of the M-power estimators. Another 1-D phase unwrapping is performed in the time domain to correct a remaining frequency offset or oscillator phase noise. The M-fold phase ambiguity is mitigated using sync-words in the packet preamble.

2.2. Description of the DADS waveform

Figure 3 Transmission chain of the DADS waveform
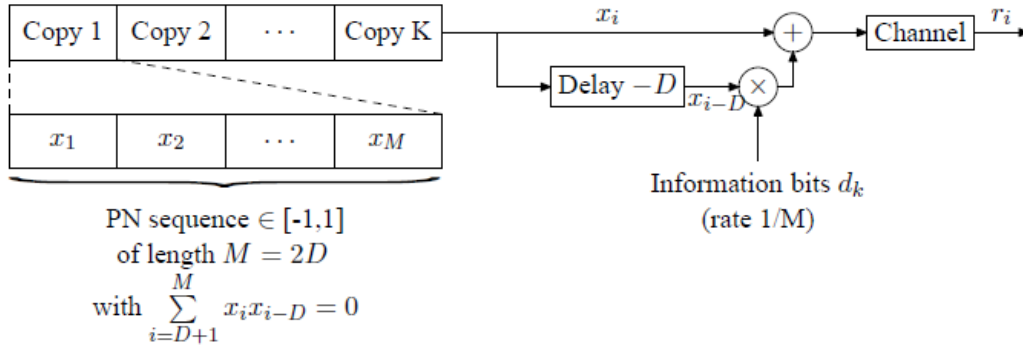
The DADS waveform has been introduced in [4]. A CR node modulates the bit sequence by the transmission chain shown in Figure 3. Assuming that K bits have to be transmitted, the PN sequence of length M is repeated K times to form the reference signal. The transmitted signal is the sum of two signals, namely the reference signal and its delayed version multiplied by the information signal.
The received signal r_i can be modelled as

$$r_i = \sum_{l=0}^{L-1} h_l (d_k x_{i-l-D} + x_{i-l}) + n_i$$

with D the delay (in chips), d_k the information bits taking values in {-1,1} with data rate $1/M$, x_i the transmitted chip of the PN sequence, n_i the AWGN with variance $N_0/2$ per dimension, L the number of taps and h_l the complex-valued channel attenuation for the lth tap. The selection of a short PN sequence whose length M is twice the delay D used in the modulation scheme ($M = 2D$) is given by [4]

$$select \{x_i\} = \begin{cases} x_i = x_{i-2D} \quad \forall i \\ \sum_{i=D+1}^{M} x_i x_{i-D} = 0 \end{cases}$$

A PN sequence satisfying this criterion can be easily generated from the 2M possible codes. The ratio between the number of codes satisfying the auto-correlation criterion and the total number of codes 2M for delays D = 2, 4, 6, 8 are 0.5, 0.375, 0.3125, and 0.2734 respectively.

Figure 4 Receive chain of the DADS waveform
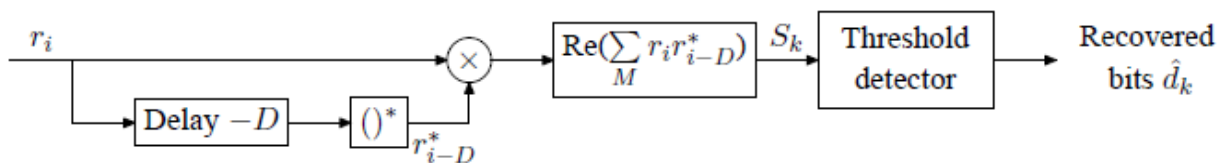
The reception chain of the CR node is shown in Figure 4. The correlator output is given by

$$S_k = Re\left(\sum_{i=(k-1)M+D+1}^{kM} r_i r_{i-D}^*\right)$$

with

$$r_i r_{i-D}^* = d_k \sum_{l=0}^{L-1} |h_l|^2 (x_{i-l-D}^2 + x_{i-l}^2) \Bigg\} \; useful \; part \; a_i$$

$$+2\sum_{l=0}^{L-1} |h_l|^2 x_{i-l} x_{i-l-D} + \sum_{l=0}^{L-1}\sum_{l'\neq l} h_l h_{l'}^* (d_k x_{i-l-D} + x_{i-l})(d_k x_{i-l'} + x_{i-l'-D}) \Bigg\} \; interference \; part \; b_i$$

$$+\sum_{l=0}^{L-1} h_l n_{i-D}^* (d_k x_{i-l-D} + x_{i-l}) + \sum_{l=0}^{L-1} h_l^* n_i (d_k x_{i-l} + x_{i-l-D}) + n_i n_{i-D}^* \Bigg\} \; noise \; part \; c_i$$

The correlator output can be divided into a useful, interference and noise parts

$$\{A_k, B_k, C_k\} = Re\left(\sum_{i=(k-1)M+D+1}^{kM} \{a_i, b_i, c_i\}\right)$$

Assuming that the correlator output approaches a Gaussian distribution, the bit error rate (BER) performance can be expressed semi-analytically as

$$BER = \frac{1}{2} E_{h_l}[Prob(S_k < 0|d_k = +1) + Prob(S_k \geq 0|d_k = -1)]$$
$$= \frac{1}{4} E_{h_l}\left[erfc\left(\frac{E[S_k|d_k = +1]}{\sqrt{2(var[S_k|d_k = +1])}}\right) + erfc\left(\frac{E[S_k|d_k = -1]}{\sqrt{2(var[S_k|d_k = -1])}}\right)\right]$$

with $erfc(.)$ the complementary error function. A_k and B_k are deterministic values. For large M, the correlator output approaches a Gaussian distribution with mean and variance

$$E[S_k] = A_k + E[B_k] + E[C_k]$$
$$var[S_k] = var[B_k] + var[C_k]$$

The integrated useful part A_k, interference part B_k and the mean of the noise part C_k are given by

$$var[B_k] = 4\sum_{l=0}^{L-1} |h_l|^4 (M-D)P_s^2 + \sum_{l=0}^{L-1}\sum_{l'\neq l} |h_l|^2 |h_{l'}|^2 (M-D)$$
$$var[C_k] = 4\sum_{l=0}^{L-1} |h_l|^2 (M-D)P_s \frac{N_0}{2} + (M-D)\frac{N_0^2}{2}$$

Knowing that a transmitted data bit is the sum of two sequences of length M, the energy per bit E_b can be written as $E_b = 2MP_s$, the derivation of the BER formula leads to the following expression [4]

$$BER = \frac{1}{2} E_{h_l}\left[erfc\left(\sqrt{\frac{\frac{M-D}{M}\sum_{l=0}^{L-1}|h_l|^2 E_b}{2N_0\Gamma}}\right)\right]$$

with

$$\Gamma = 1 + \frac{\sum_{l=0}^{L-1}|h_l|^4 E_b}{\sum_{l=0}^{L-1}|h_l|^2 MN_0} + \frac{MN_0}{2\sum_{l=0}^{L-1}|h_l|^2 E_b} + \frac{\sum_{l=0}^{L-1}\sum_{l' \neq l}|h_l|^2 \left|h_{l'}\right|^2 E_b}{\sum_{l=0}^{L-1}|h_l|^2 MN_0}$$

3. Description of the CR demonstrator and results

Figure 5 Parameters chosen for the multichannel DAA-OFDM and DADS waveforms

Multichannel DAA-OFDM parameters		DADS parameters	
FFT size	512	PN sequence length	4
CP size	128	Packet length (bits)	63040
Number of modulated sub-carriers	416	Sampling rate (Msps)	2
Number of channels	4	Slot duration (ms)	126.08
Number of sub-carriers per channel	104	FDD mode maximum throughput (kbps)	500.00
Packet length (bits)	81920	TDD mode maximum throughput (kbps)	250.00
Constellation per sub-carrier	QPSK		
Sampling rate (Msps)	2		
Slot duration (ms)	126.08		
FDD mode maximum throughput (kbps)	649.75		
TDD mode maximum throughput (kbps)	324.87		

The multichannel DAA-OFDM and the DADS waveforms are chosen for the demonstrator. The parameters chosen for the multichannel DAA-OFDM and DADS waveforms are given in Figure 5.

Figure 6 Simulated BER performance of the multichannel DAA-OFDM and DADS waveforms
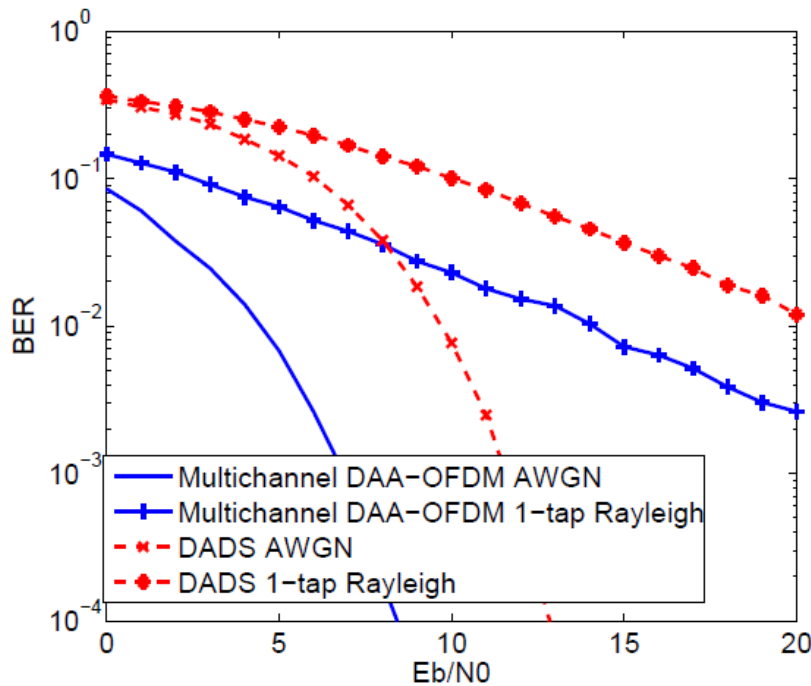

Figure 6 shows the simulated BER performance of the multichannel DAA-OFDM waveform and the DADS waveform in AWGN channels and 1-tap Rayleigh channels. One can observe that the multichannel DAA-OFDM waveform has better BER performance than the DADS waveform by 4 dB at BER 10^{-4}.

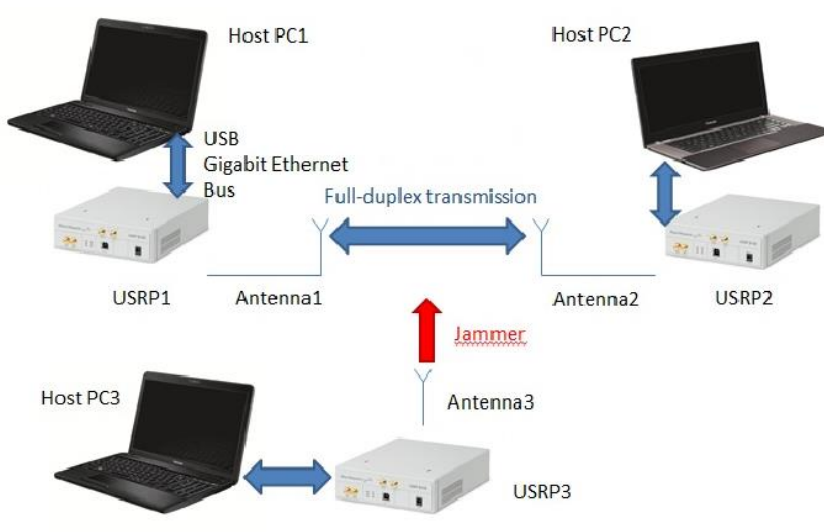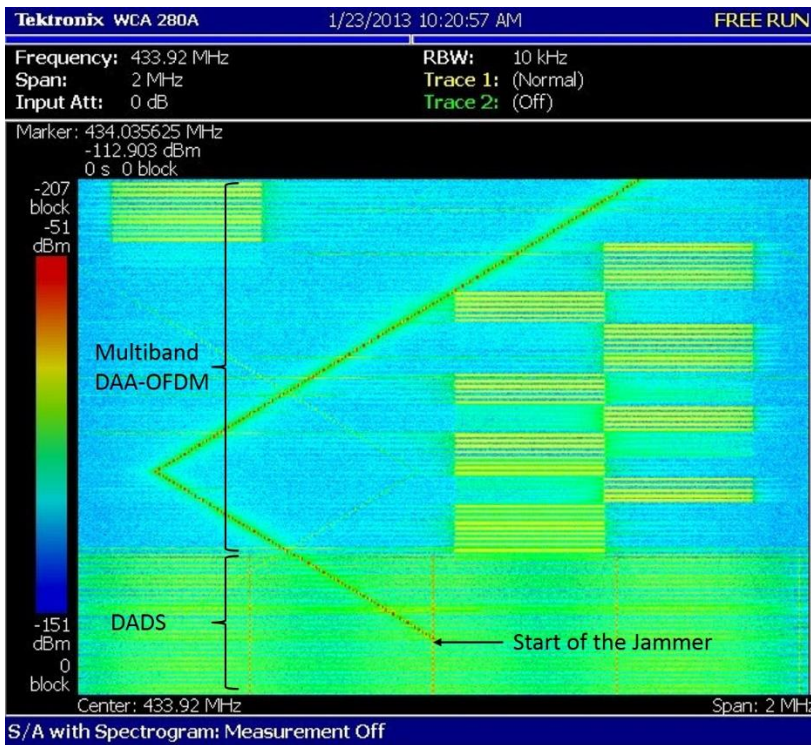## Figure 7 Setup used for the demonstrator

Figure 7 shows the CR demonstrator setup. In this setup, a jammer perturbs the data transmission between two CR nodes. The first CR node has a quad-core CPU@2.9 GHz with 8 GB RAM and the second CR node has a quad-core CPU @2.4 GHz with 4 GB RAM.

Figure 8 Spectrogram showing the cognitive capability of the CR nodes

The CR nodes operate at 433.92 MHz. The CR nodes can use either the multichannel DAA-OFDM waveform or the DADS waveform in a TDD mode. Figure 8 shows the spectrogram of the CR nodes when a jammer perturbs the data transmission. At the beginning of the demonstration, the CR nodes use the DADS waveform. At a certain moment, a sweeping jammer perturbs the transmission and the throughput of both users drops. When the user throughput drops under a particular threshold (1 kbps), the CR nodes switch from the DADS waveform to the multichannel DAA-OFDM waveform automatically while maintaining communication. The multichannel DAA-OFDM waveform adjusts dynamically the channel used for transmission and mitigates interference by sensing its operational electromagnetic environment. Therefore, whenever the jammer perturbs the channel used for transmission, the multichannel DAA-OFDM waveform is able to jump to another channel while maintaining communication.

In the case of reactive jammers, frequency hopping can be enabled by a predefined hopping sequence only known to the CR nodes. The USRP RF frontend allows to perform frequency hopping over a large frequency range from 70 MHz to 6 GHz. Some tests with the USRP have shown that the maximum frequency tuning time is about 700 ns, giving a maximum limit on the hop rate of 1500 hops/s.

During demonstration measurements of the multichannel DAA-OFDM and the DADS waveforms in a TDD mode, we have observed that the averaged throughput corresponds to the maximum throughput 250 kbps for the DADS waveform when streaming either from the first CR node to the second CR node or from the second CR node to the first CR node. However, the averaged throughput for the multichannel DAA-OFDM waveform is less than the maximum throughput 324.87 kbps from the first CR node to the second CR node (64 kbps) and from the second CR node to the first CR node (160 kbps). The difference between the maximum throughput and the averaged throughput can be explained by three factors. The first factor is the processing power of the CR nodes. The second factor is the larger complexity of the receivers compared to the transmitters. The third factor is the larger complexity of the multichannel DAA-OFDM

waveform compared to the DADS waveform. Due to these three factors, the two CR nodes are not able to process every packet in 252.16 ms. At the transmit side, the same packet can be sent for several frame periods. At the receive side, some packets can be missed. Therefore, the complexity of CR waveforms is a very important issue when they are implemented on SDR platforms especially when using general purpose processors (GPP).

Figure 9 Throughput results for the multichannel DAA-OFDM and DADS waveforms

Sampling rate (Msps)	Multichannel DAA-OFDM demonstration results		DADS demonstration results	
	FDD mode maximum throughput (kbps)	Averaged throughput	FDD mode maximum throughput (kbps)	Averaged throughput
2	649.75	87.00	500.00	450.00
1	324.88	90.00	250.00	231.00
0.5	162.44	96.00	125.00	113.00
0.25	81.22	79.00	62.50	58.00

Figure 9 shows some throughput results for the multichannel DAA-OFDM and DADS waveforms when considering different sampling rates in a FDD mode. One can observe that the averaged throughput of the DADS waveform is close to the maximum throughput for any sampling rate. There is a small decrease in averaged throughput compared to the maximum throughput because the two CR nodes are not able to process every packet in 126.08 ms. This small decrease does not appear in a TDD mode (averaged throughput=maximum throughput) because the processing thread has enough time to process every packet in 252.16 ms. For high sampling rates, the averaged throughput of the multichannel DAA-OFDM waveform is lower than the maximum throughput. However, for lower sampling rates, the difference between the averaged throughput and the maximum throughput decreases. Therefore, more complex waveforms such as the multichannel DAA-OFDM waveform can still be used using GPP either at lower sampling rates or by defining a frame with multiple slot periods such as in a TDD mode or in a time division multiple access (TDMA) to increase the time in which the packet can be processed.

4. Conclusion

CogWave is an open-source software framework aiming at developing cognitive radio (CR) waveforms. Multiple waveforms have been implemented in CogWave, such as the multichannel DAA-OFDM waveform, the DADS waveform, and GNU Radio waveforms. CogWave provides the means to implement different CR waveforms and to develop rules to switch between different CR waveforms during run-time according to the user needs and the electromagnetic environment. A description of a CR demonstrator is given, in which a jammer perturbs the data transmission between two CR nodes. It is shown that when the throughput drops under a predefined threshold, the CR nodes switch from the DADS waveform to the multichannel DAA-OFDM waveform automatically while maintaining communication. Due to the low

complexity of the DADS waveform, the averaged throughput is close to the maximum throughput for sampling rates up to 2 Msps. For more complex waveforms such as the multichannel DAA-OFDM waveform, the averaged throughput is close to the maximum throughput at lower sampling rates (0.25 Msps). Therefore, the parameters of CR waveforms should be properly adjusted to take into account the processing time vs the acquisition time when implemented on SDR platforms especially when using general purpose processors (GPP).

5. References

[1]   J. Mitola III, "Cognitive radio: making software radios more personal," IEEE Personal Communications, vol. 6, no. 4, pp. 13–18, Aug. 1999.

[2]   "Cogwave: Open-source software framework for cognitive radio waveforms," 2013. [Online]. Available: https://github.com/vlenircissrma/CogWave

[3]   V. Le Nir and B. Scheers, "Implementation of an adaptive OFDMA PHY/MAC on USRP platforms for a cognitive tactical radio network," in Military Communications and Information Systems Conference (MCC'2012), Gdansk, Poland, Oct. 2012.

[4]   ——, "DADS with short spreading sequences for high data rate communications or improved BER performance," in Military Communications and Information Systems Conference (MCC'2013), Saint-Malo, France, Oct. 2013.

[5]   GNU Radio. [Online]. Available: http://www.gnuradio.org

[6]   OMNeT++ Network Simulation Framework. [Online]. Available: http://www.omnetpp.org

[7]   Network Simulator ns-3. [Online]. Available: http://www.nsnam.org/

[8]   D. Danev, E. Axell, and E. G. Larsson, "Spectrum sensing methods for detection of DVB-T signals in AWGN and fading channels," in Proceedings of the IEEE 21st International Symposium on Personal Indoor and Mobile Radio Communications (PIMRC'2010, Istanbul, Turkey, Sep. 2010.

[9]   J.-J. van de Beek, M. Sandell, and P. O. Borjesson, "ML Estimation of Time and Frequency Offset in OFDM Systems," IEEE Transactions on Signal Processing, vol. 45, no. 7, pp. 1800–1805, Jul. 1997.

[10]   C. N. Georghiades, "Blind Carrier Phase Acquisition for QAM constellations," IEEE Transactions on Communications, vol. 45, no. 11, pp. 1477–1486, Nov. 1997.

[11]   H. Meyr, M. Moeneclaey, and S. A. Fechtel, Eds., Digital Communications Receivers: Synchronization, Channel Estimation, and Signal Processing. John Wiley and Sons, 1998.